What determines tree mortality in dry environments?
a multi-perspective approach

Michael Dorman,[1,7] Tal Svoray,[1] Avi Perevolotsky,[2] Yitzhak Moshe,[3] and Dimitrios Sarris[4,5,6]

[1]*Department of Geography and Environmental Development, Ben-Gurion University of the Negev, Beer-Sheva 84105 Israel*
[2]*Department of Agronomy and Natural Resources, Agricultural Research Organization, Volcani Center, Bet Dagan 50250 Israel*
[3]*Keren Kayemeth LeIsrael, Southern Region, Gilat Afforestation and Soil Conservation, Gilat Doar-Na Hanegev 85410 Israel*
[4]*Faculty of Pure and Applied Sciences, Open University of Cyprus, 2252 Latsia, Nicosia, Cyprus*
[5]*Department of Biological Sciences, University of Cyprus, 1678 Nicosia, Cyprus*
[6]*Division of Plant Biology, Department of Biology, University of Patras, 265 00 Patras, Greece*

Abstract. Forest ecosystems function under increasing pressure due to global climate changes, while factors determining when and where mortality events will take place within the wider landscape are poorly understood. Observational studies are essential for documenting forest decline events, understanding their determinants, and developing sustainable management plans. A central obstacle towards achieving this goal is that mortality is often patchy across a range of spatial scales, and characterized by long-term temporal dynamics. Research must therefore integrate different methods, from several scientific disciplines, to capture as many relevant informative patterns as possible.

We performed a landscape-scale assessment of mortality and its determinants in two representative *Pinus halepensis* planted forests from a dry environment (~300 mm), recently experiencing an unprecedented sequence of two severe drought periods. Three data sources were integrated to analyze the spatiotemporal variation in forest performance: (1) Normalized Difference Vegetation Index (NDVI) time-series, from 18 Landsat satellite images; (2) individual dead trees point-pattern, based on a high-resolution aerial photograph; and (3) Basal Area Increment (BAI) time-series, from dendrochronological sampling in three sites.

Mortality risk was higher in older-aged sparse stands, on southern aspects, and on deeper soils. However, mortality was patchy across all spatial scales, and the locations of patches within "high-risk" areas could not be fully explained by the examined environmental factors. Moreover, the analysis of past forest performance based on NDVI and tree rings has indicated that the areas affected by each of the two recent droughts do not coincide.

The association of mortality with lower tree densities did not support the notion that thinning semiarid forests will increase survival probability of the remaining trees when facing extreme drought. Unique information was obtained when merging dendrochronological and remotely sensed performance indicators, in contrast to potential bias when using a single approach. For example, dendrochronological data suggested highly resilient tree growth, since it was based only on the "surviving" portion of the population, thus failing to identify past demographic changes evident through remote sensing. We therefore suggest that evaluation of forest resilience should be based on several metrics, each suited for detecting transitions at a different level of organization.

Key words: aerial photography; Aleppo pine; dendrochronology; drought; Landsat; Pinus halepensis; remote sensing; semiarid; tree rings.

Introduction

Drought-induced forest mortality

Changes in climate are taking place at an increasing rate across the globe, and are likely to continue into the future (Mora et al. 2013). The uncertainty of how forest ecosystems will respond to projected climatic changes is an on-going challenge. For instance, the physiological mechanisms through which drought drives tree mortal-ity are a rapidly growing research interest (McDowell et al. 2008, 2011, Anderegg et al. 2012). However, mechanistic understanding of tree mortality processes is yet insufficient for prediction of timing, or spatial pattern, of tree die-off events (McDowell et al. 2011, 2013a). Therefore, observational studies are essential for documenting the decline events that are already underway (Allen et al. 2010), understanding their determinants, and developing forest management plans to ensure that forest ecosystems services are sustained (Anderegg et al. 2013a). Particularly, factors and processes determining when and where mortality events will take place within the wider landscape are poorly

understood (Allen et al. 2010, Dwyer et al. 2010, Brouwers et al. 2013a, Clifford et al. 2013).

A multi-perspective observation approach; motivation

Mortality processes are often patchy across a range of spatial scales (Breshears et al. 2011, Michaelian et al. 2011, Macfarlane et al. 2013) and are characterized by long-term temporal dynamics (Bigler et al. 2007, Galiano et al. 2011, Anderegg et al. 2013b). Research therefore must necessarily integrate several scientific disciplines and their respective methods (Hicke and Zeppel 2013, McDowell et al. 2013b) to capture as many relevant informative patterns as possible, such as lagged drought effects on mortality (Bigler et al. 2007) or spatial clustering of dead trees (Liu et al. 2007). In particular, for better understanding the spatial pattern of mortality at regional scales, it is necessary to integrate explicit measurements of ecosystem functioning indicators in the field (Breshears et al. 2009b) with remotely sensed data. The latter are essential to fill data gaps, both in terms of extensive spatial coverage and the ability to look back in time (Rich et al. 2008, Garrity et al. 2013).

The Normalized Difference Vegetation Index (NDVI) is a measure of vegetation greenness and moisture content (Tucker 1979, Pettorelli et al. 2005, Stimson et al. 2005) that is often used as an inclusive measure of forest physiological performance in response to environmental change (Volcani et al. 2005, Dorman et al. 2013b). However, the highest spatial resolution of currently available long-term data (30 m, in Landsat) is insufficient to interpret change in terms of structural and demographic processes the forest goes through (Macfarlane et al. 2013). Therefore, it is necessary to complement remotely sensed greenness trends with measurements of individual tree performance (e.g., radial growth rate) and demographic processes (e.g., mortality rate).

On the one hand, high-resolution aerial photographs, where individual trees are detectable, may provide spatially extensive information on population density changes and mortality rates (Shimazaki et al. 2011, le Polain de Waroux and Lambin 2012, Dorman et al. 2013a, Baguskas et al. 2014), although for sparse and irregularly spaced points in time. On the other hand, the information recorded in tree rings can be dated to construct annual-resolution time series, expressing physiological state of individual sampled trees, although usually covering a limited spatial extent (but see Rozas and Olano 2013). Thus, each of the above-mentioned approaches contributes a unique piece of information, essential for addressing the complex problem at hand. Many previous efforts to examine environmental determinants of forests' response to drought have, however, used a single approach (e.g., satellite remote sensing [Volcani et al. 2005, Yuhas and Scuderi 2009, Vacchiano et al. 2012], aerial photography [Allen and Breshears 1998, Fensham et al. 2005, Clifford et al.

2011], and field or dendrochronological measurements [Suarez et al. 2004, Gitlin et al. 2006, Vila-Cabrera et al. 2013]). Recently, several studies have successfully combined dendrochronological methods with remote sensing to provide a more comprehensive perspective on forest mortality dynamics (Lopatin et al. 2006, Linares et al. 2009a, Babst et al. 2010, Beck et al. 2011, Berner et al. 2011, Lloyd et al. 2011, Kharuk et al. 2013).

The case study; Pinus halepensis-*planted forests in a semiarid region*

Pinus halepensis is considered the most drought-tolerant of the Mediterranean pine species (Schiller 2000). Planted forests of this species in the semiarid region of Israel, established primarily for their aesthetic values and used for recreation (Perevolotsky and Sheffer 2009), represent one of the most extreme environments in which the species occurs (Schiller and Atzmon 2009, de Luis et al. 2013). Following an unprecedented sequence of drought periods (1998–2000 and 2005–2011), a steep decline in NDVI (Dorman et al. 2013b), as well as increased mortality (Schiller et al. 2005, Dorman et al. 2013a, Klein et al. 2014), were observed in the planted *P. halepensis* forests occupying the dry edge of the Mediterranean region in Israel (<350 mm of annual rainfall). The latter is one of several analogous observations made in *P. halepensis* s.l. forests around the Mediterranean (Sarris et al. 2007, Vicente-Serrano et al. 2010, Girard et al. 2011, 2012), as well as at the dry edges of distribution of other tree species (Linares et al. 2009a, Matyas 2010, Vila-Cabrera et al. 2011). However, the extent, spatial pattern, and association of mortality with environmental conditions have not been systematically investigated.

Due to the harsh climate, natural regeneration is negligible in the *P. halepensis* planted forests that receive <400 mm of rainfall (Osem et al. 2009, 2013), making forest mortality irreversible without replanting. Analogously, mortality is considered "irreversible" in natural semiarid forests, where it may take decades for a pre-drought extent of mature canopy overstory to develop (Breshears et al. 2011). Understanding the spatial pattern of mortality is therefore crucial for preparing management guidelines designed for these forests, and semiarid forest ecosystems elsewhere, which are expected to experience increasing drought stress under global climate change. Moreover, thanks to the relative homogeneity and the artificial "placement" (by means of planting) of the studied system beyond the natural distribution limit of the species (~450 mm of rainfall [Schiller 2000, Liphschitz and Biger 2001]), it may serve as an (unintended) experiment demonstrating trends and processes that may occur at *natural* forest xeric limits in the future.

A high-resolution aerial photograph of the drought-affected area was taken in winter 2011/2012, immediately following the peak of a drought period (2005–2011). Identification of individual dead trees in the

photograph, the feasibility of which has been previously demonstrated (Dorman et al. 2013a), has been used to systematically map mortality pattern in two representative forests. Forest age (Dorman et al. 2012), topographic aspect (Dorman et al. 2013a), past (preplantation) cultivation indicative of deeper soil (Y. Moshe, *personal observation*), and tree density were examined concerning tree mortality. The last parameter is of particular importance in forest management, since thinning is considered the main tool for enhancing forests' adaptive capacity to withstand drought stress (Linares et al. 2009b, Kerhoulas et al. 2013, Sánchez-Salguero et al. 2013). A series of Landsat satellite images and dendro-ecological field data provided complementary information for characterizing the spatiotemporal variation in forest performance.

Aim and study questions

The aim of this paper was to perform a landscape-scale assessment of *P. halepensis* mortality pattern and its determinants in a dry environment using a multi-perspective approach. From the applied point of view of forest management, the results of the study are ultimately intended to provide knowledge for projecting future impacts of climate change on semiarid planted forests, and for how (and to what extent) the effects may be alleviated. The specific study questions were:

1) What was the spatial pattern (i.e., clustered, random, or regular) of dead trees occurrence within the forests following a severe drought?
2) How did biotic (age, density) and abiotic (topographic aspect, soil depth) conditions influence tree mortality risk?
3) In what way is the forested area divided into distinctive zones characterized by unique past performance trajectories? Are these associated with environmental conditions and with tree mortality risk?

Materials and Methods

Study area

The studied area included all 6.6 km^2 of *P. halepensis*-planted stands in Lahav and Dvira forests (Fig. 1; Israel Forest Service). The climate is semiarid (average annual rainfall of ~300 mm; Fig. 2), and highly seasonal (five consecutive months with <2.5 mm rainfall depth). The forests are located almost exclusively on Brown Lithosol and Colluvial-Alluvial Loess (93% of area) and on Light Brown Loess Soils and Brown Lithosol (7%) (Dan et al. 1970). From personal observations and communication with foresters it was apparent that: (a) dead trees are removed within a short time, and (b) the routine forest management includes thinning once every 12–15 years.

Three sites were randomly selected within the area of Lahav and Dvira forests (Fig. 1) for dendrochronological sampling for tree growth. All sites were located on

south-facing slopes, and were of similar age (43–45 years old in 2012).

Mapping forest mortality and environmental conditions

Forest *mortality* and *trees density* were measured using a high-resolution (0.25 m) orthophoto from the winter of 2011/2012. Dead trees were identified and marked by visual interpretation of the aerial photograph, where they were clearly distinguishable due to their gray/reddish color, compared with the green living trees (Appendix A: Figs. A1, A2; see also Fig. S1 in Dorman et al. 2013a). To measure total (dead + living trees) tree density (Appendix A: Fig. A3), and subsequently mortality fraction (dead trees/total number of trees), the living trees were counted as well, within a subset of the forest area. That subset consisted of a randomly selected 10% of the 6070 grid cells (coinciding with Landsat pixels, see *Materials and methods: Satellite remote sensing*) covering the whole forest area. Forest *age* in 2012 (Appendix A: Fig. A3) was calculated based on planting dates GIS layer (acquired from the Israel Forest Service).

The area was classified to north- and south-facing *topographic aspects* (Appendix A: Fig. A3) using the 25-m resolution Digital Elevation Model (DEM) layer of Israel (Hall and Cleave 1988). Classification was based on incoming solar radiation estimate (Fu and Rich 2002, Dorman et al. 2013a). Thus, we use the terms "northern" and "southern" aspects not in their narrow sense (slopes facing the north or the south, respectively), but as labels for the classification of the studied area into two distinct categories differing in their radiation load.

Historical aerial photographs were used to delineate previously cultivated fields (i.e., traditional rain-fed cereal plots) indicative of *deep soils*. The fields could be identified by their bright and "smooth" texture with sharp, straight boundaries (Appendix A: Fig. A3), compared with the rocky terrain which is unsuitable for cultivation and used mainly for grazing. Ten images of the Lahav and Dvira forests (Appendix A: Fig. A4), taken during winter–spring 1945, were geo-referenced to the 2012 images based on position of invariant features such as rock outcrops. Geo-referencing was performed using a second-order polynomial model and >20 control points for each image. Geo-referencing Root Mean Square Error (RMSE) was between 2.4 and 4.6 m (Appendix A: Table A1). A given 30 × 30 m^2 pixel was considered as "deep soil" if >90% of its area was covered by fields.

Satellite remote sensing

Eighteen Landsat satellite images (16 from Landsat-5 TM, 2 from Landsat-7 ETM+; Appendix B: Table B1), from the period 1994–2012 (one image per year, except for 2002), were used to calculate NDVI time-series for the 6070 pixels of 30 × 30 m^2 that are completely within forest polygons (Appendix B: Fig. B1). All images were acquired during a relatively short time period at the end
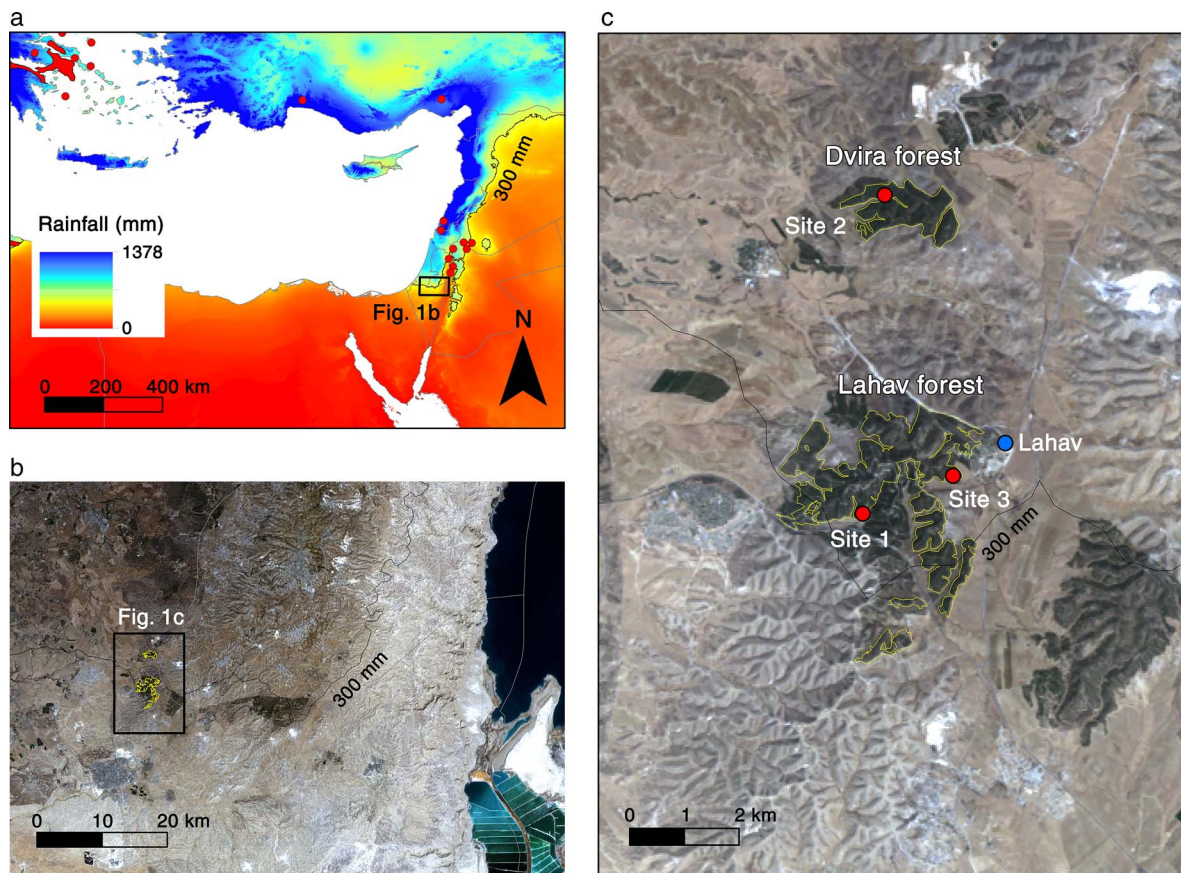
Fig. 1. Location of the study area within the semiarid climatic zone, bordering the more humid Mediterranean climate to the north and the more arid Negev desert to the south. In (a), average annual rainfall amounts for the period 1950–2000 (data from http://www.worldclim.org/) are shown as background colors and natural distribution range of *Pinus halepensis* is shown in red (data from http://www.euforgen.org/distribution-maps). Lahav and Dvira forests locations, respectively to the 300-mm rainfall line, are shown in (b) and (c), where the background is an RGB Landsat-5 satellite image from 2003. The blue data point in panel (c) marks the location of "Lahav" meteorological station (Fig. 2); the red data points mark the locations of dendrochronological sampling sites.

of the dry season (8 September–16 October), when annual vegetation is completely dry (Appendix A: Fig. A1; [Svoray and Karnieli 2011, Shafran-Nathan et al. 2013]) and soil water content is most temporally stable (Raz-Yaseef et al. 2012). Since perennial vegetation (other than the *P. halepensis* trees) and natural regeneration of *P. halepensis* in this area are negligible due to aridity (Appendix A: Fig. A1) (Osem et al. 2009, 2013), the NDVI signal can be fully attributed to the greenness and water content of the planted *P. halepensis* tree canopy. Images were subjected to geo-referencing, followed by radiometric and atmospheric calibration, using standard methods (see Dorman et al. 2013b for details).

Since 2003, Landsat-7 ETM+ has been operating without the Scan Line Corrector (SLC), which compensates for the forward motion of the satellite during image acquisition. Data collected at the SLC-off mode have gaps in a systematic wedge-shaped pattern; however, spatial and spectral qualities of the remaining portions of the imagery are not diminished (Wulder et al. 2008, Chen et al. 2011). The issue applies only to our 2012 Landsat-7 ETM+ image, which does not cover ~22% of studied area due to the SLC-off mode (Appendix B: Fig. B1). To eliminate any potential bias due to the incomplete NDVI coverage for 2012, only the period 1994–2011 was considered for spatiotemporal analysis of NDVI data (see *Materials and methods: Statistical methods*. However, since the 2012 image did cover the three dendrochronological sampling sites, it could still be used in the comparison between remote sensing and tree rings inferences regarding drought response (see Fig. 8).

Non-forest areas (roads, buildings, etc.) were manually digitized, and pixels where >10% of the area was non-forest were excluded from the analysis. The final sample sizes were 4839 pixels of 30 × 30 m^2 for spatiotemporal clustering of NDVI, and 471 pixels for evaluation of environmental effects on mortality.
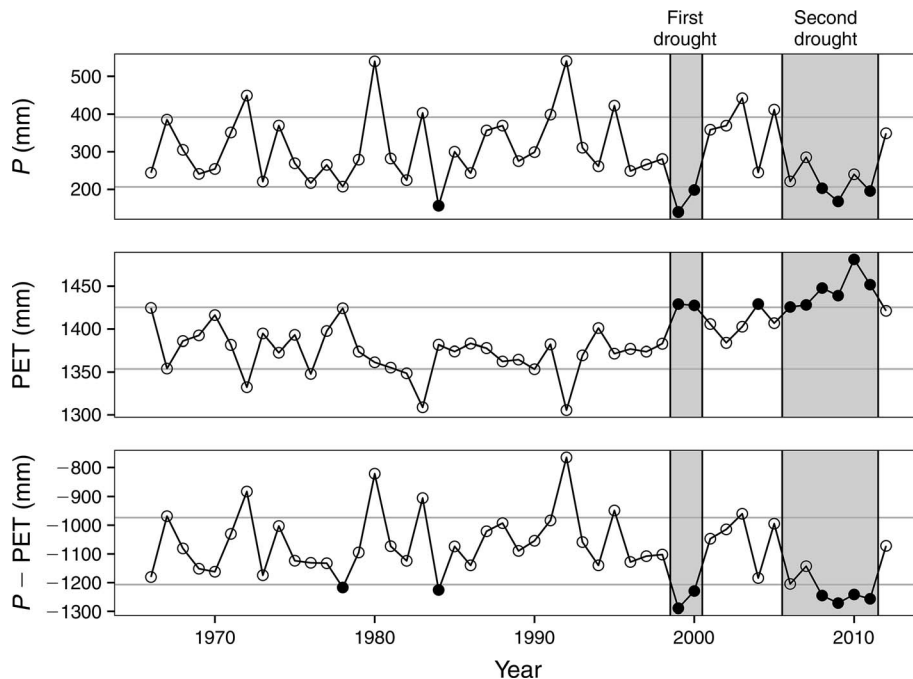
Fig. 2. Annual precipitation (P), potential evapotranspiration (PET), and water balance ($P -$ PET) in Lahav during 47 years (1966–2012). Horizontal lines mark the range of the average ± 1 SD for each variable. Values outside of this range towards drought conditions (low P, high T, low $P -$ PET), are marked in black.

Dendrochronological methods

Dendrochronological sampling was conducted during autumn 2011–spring 2012. In each of the three sites, 30 living, unsuppressed, i.e., not overshadowed by their neighbors, trees were randomly selected. Two wood cores were extracted from opposite sides of each tree at breast height using an increment borer. Cores were sanded using increasingly fine sanding paper until tree rings were clearly visible under a binocular microscope. Tree ring width (TRW) was measured to an accuracy of 0.01 mm using a LINTAB 6 measuring device (Rinntech, Heidelberg, Germany). Five trees with damaged cores or undatable missing rings were removed from the analysis. Finally, TRW values were converted to basal area increment (BAI) values (Biondi and Qeadan 2008), and average BAI chronologies were calculated per site. Structural characteristics of the sites (tree dimensions, density, and mortality) are provided in Appendix C.

Climate data

To characterize climatic conditions in the studied area, precipitation (P), minimum temperature (Tmin), and maximum temperature (Tmax) daily data for the period 1966–2012 were obtained from the standard meteorological station "Lahav" bordering Lahav forest (Fig. 1). Missing values (6%) of Tmin and Tmax were filled based on data from "Beer-Sheva" station (16 km to the south from "Lahav") using linear regression. The agreement between the data series from the stations was very high, producing R^2 values of 0.99 for Tmax, and

0.88 for Tmin, based on ~17 000 days when both stations operated. Potential evapotranspiration (PET) was estimated based on Tmin, Tmax, and latitude using the Hargreaves method (Fig. 2) (Hargreaves 1994).

Annual rainfall amount was elected as the most important climatic variable affecting forest growth in the studied region, following a previous systematic examination (Dorman et al., *in press*). It was therefore used to evaluate the degree to which climatic conditions determine NDVI and tree growth rates.

Statistical methods

Two main issues of interest in the analysis of spatial point patterns concern the distribution of events (dead trees, in our case; Appendix A: Fig. A2) in space, and the existence of possible interactions between them (Bivand et al. 2008). The former was examined by fitting linear models to the tree mortality data; the latter, by comparing Ripley's K-function (Ripley 1977) values to those expected under complete spatial randomness (CSR; i.e., a homogenous Poisson process). Ripley's K-function analysis (Fig. 3) is based on the concept that if λ is the density of events per unit area, the expected number of points in a circle with radius t centered on a randomly chosen point is $\lambda K(t)$, where $K(t)$ is a function of t that depends on the spatial pattern of the points (Fortin and Dale 2005).

The statistic $\hat{K}(t)$ is an estimate of $K(t)$. Its value under CSR is $K(t) = \pi t^2$; values $\hat{K}(t) - \pi t^2 > 0$ indicate clustering, while values $\hat{K}(t) - \pi t^2 < 0$ indicate a regular

pattern (Fortin and Dale 2005). Random simulations (e.g., producing 99 point patterns where the events, dead trees, are randomly placed within the studied area) were performed to interpret the type of interaction (i.e., clustered, random, or regular pattern) and its scale (i.e., manifestation over short/long distances).

The effects of environmental conditions on the proportion of dead trees were evaluated using a binomial Generalized Linear Model (GLM; Figs. 4, 5; Appendix D). The dependent variable was the dead to total trees count ratio (i.e., mortality proportion) in each 30×30 m^2 pixel. The independent variables were age, density, aspect, and soil depth, and all of their two-way interactions. The latter two were handled as dummy variables, representing two categories (southern vs. northern, and deep soil vs. non-deep soil). A model selection procedure (Johnson and Omland 2004), based on the Akaike Information Criterion (AIC) (Akaike 1974), was employed to select the final model (Appendix D).

To test whether the two consecutive drought events affected either the same or different areas within the forests, we have both visually compared decline magnitudes (i.e., ΔNDVI) maps (Fig. 6), and statistically tested whether a correlation existed between the ΔNDVI values (Appendix E).

An exploratory method of organizing spatiotemporal data is to develop clusters of these data (Chapman et al. 2012, Plant 2012). K-means cluster analysis, using the algorithm of Hartigan and Wong (1979), was applied to examine the spatial pattern of NDVI change through time (Fig. 7). The data for each pixel were standardized to a mean of zero and standard deviation of one (Anderson et al. 2010), to remove differences due to site quality (e.g., north-facing slopes generally have higher NDVI values than south-facing slopes) and concentrate only on the differences in the temporal sequence and direction of NDVI changes. It is important to note that no spatial information is used in the algorithm; each pixel is treated as an independent observation. The optimal number of clusters was determined as four by visually examining the plot of within-groups sums of squares as function of clusters number (Appendix F: Fig. F1) (Hothorn and Everitt 2009).

The resulting four clusters were arbitrarily labelled from 1 to 4 according to mortality level (1 is highest, and 4 is lowest). Dendrochronological sampling sites were consequently also labelled from 1 to 3, since each site was located within one of the 1–3 clusters. Results were visually evaluated in terms of clusters' spatial distribution (Fig. 7a), their average NDVI trajectories (Fig. 7b), and their association with environmental conditions and mortality rates (Appendix F: Table F1). Linear discriminant analysis was used to assess separation of the clusters (Fig. 7c).

The effects of annual rainfall on BAI and NDVI for the dendrochronological sampling sites were determined
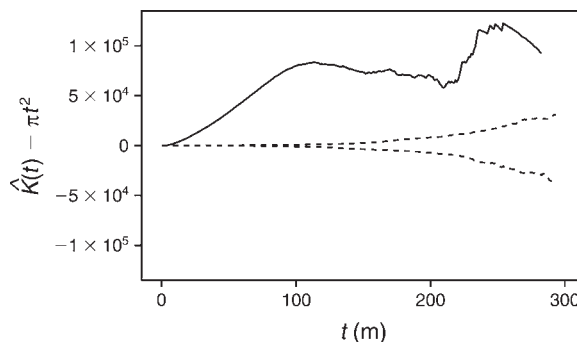

Fig. 3. Ripley's K function minus its expected value at Complete Spatial Randomness (CRS), as function of distance, for the dead *P. halepensis* trees point pattern (Appendix A: Fig. A2). Empirical values (solid line) above or below the envelope produced by 99 random simulations (dashed lines) indicate that dead trees were significantly aggregated or significantly regular, respectively. In the present case dead trees were spatially aggregated across all spatial scales. See *Materials and methods: Statistical methods.*

using linear regression (Fig. 8), based on the common period of data availability (1994–2012, excluding 2002).

Statistical analyses were conducted in R (R Development Core Team 2013). Atmospheric correction of Landsat images was done with the "landsat" package (Goslee 2011). Ripley's K-function analysis was done using package "spatstat" (Baddeley and Turner 2005). Package "MASS" (Venables and Ripley 2002) was used for linear discriminant analysis. Packages "ggplot2" (Wickham 2009) and "lattice" (Sarkar 2008) were used for visualization.

RESULTS

Spatial pattern of dead trees occurrence

A total of 8233 dead trees (Appendix A: Fig. A2) were identified within the studied forests area, giving an average density of 12.52 dead trees/ha. However, the spatial distribution of dry trees was markedly nonrandom. According to Ripley's K-function, significant clustering ("attraction") of dead trees occurred at all spatial scales (Fig. 3). Namely, dead trees usually occurred near other dead trees, and patches of dead trees near other such patches.

Environmental determinants of mortality

The average proportion of dead trees was 5%; however, mortality was highly variable in space (Fig. 5), being either zero (in 70% of the forest area) or anywhere between 0 and 90% (in the remaining area). Mortality proportion was significantly affected by all four examined factors (Appendix D: Table D1); while three of the effects were acting in the expected direction, the fourth one (trees density) was not. Visualization of model predictions (Fig. 4) revealed that age effect on mortality was positive (higher mortality in older forest stands), density effect was negative (higher mortality in sparser stands), south-facing aspect effect was positive
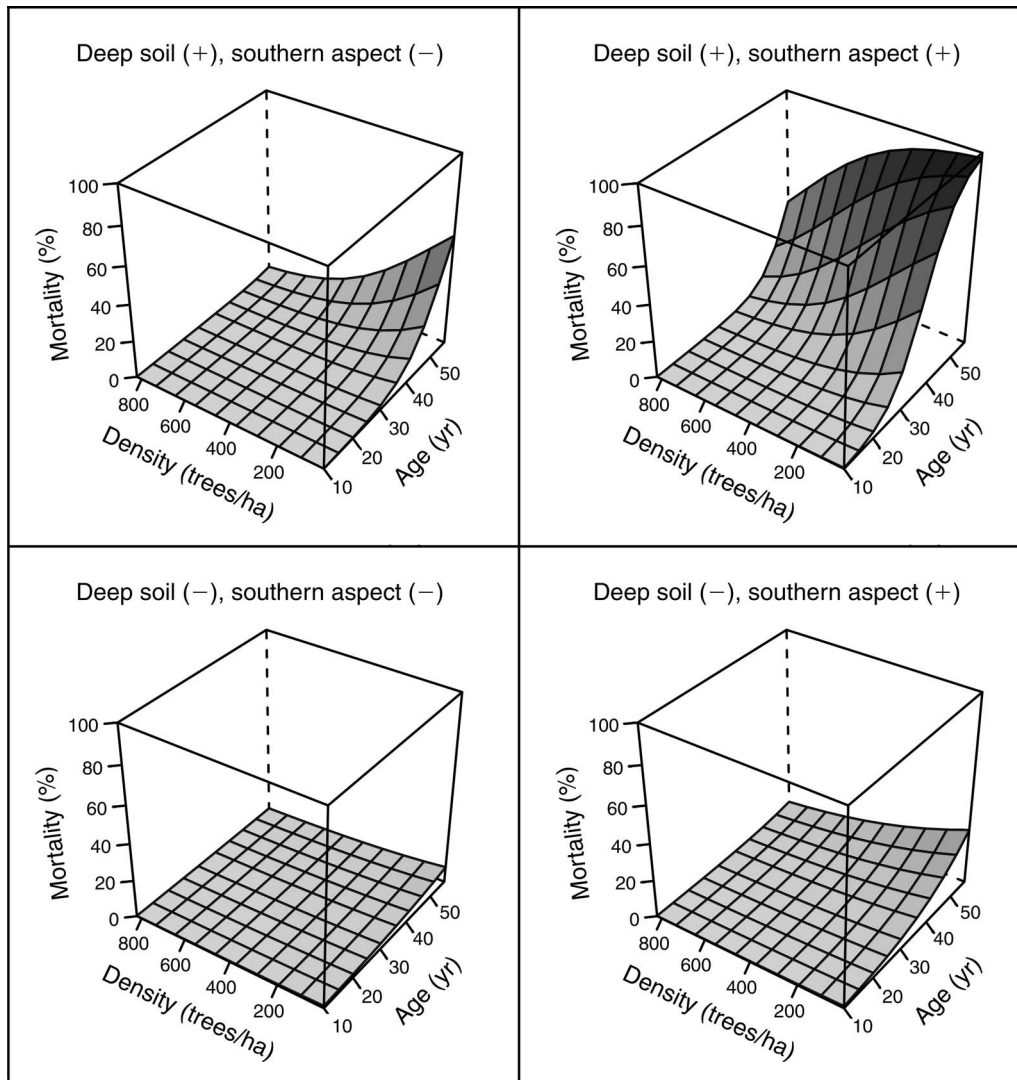
F<small>IG</small>. 4. Predicted mortality proportions as a function of tree density, age, topographic aspect, and soil depth, based on a Generalized Linear Model (GLM; Appendix D: Table D1).

(higher mortality on south-facing slopes), and deep soil effect was positive (higher mortality on deeper soils). The model explained 23.0% of variation in mortality proportions. While areas of relatively elevated mortality risk could be identified, the fine-grained patchiness in mortality was not captured using the examined factors (Fig. 5).

First vs. second drought effects

A weak negative correlation was found between the change in NDVI during the first ($\Delta NDVI_{first} = NDVI_{2000} - NDVI_{1998}$) and second ($\Delta NDVI_{second} = NDVI_{2011} - NDVI_{2005}$) droughts (Pearson correlation coefficient = −0.08, $P < 0.001$; Appendix E). A visual inspection has confirmed that the two droughts affected different regions within the forest (Fig. 6). For example, the areas where $\Delta NDVI_{first} < -0.1$ and $\Delta NDVI_{second} <$ −0.1 were 30.0% and 21.1% of the entire forested area, respectively; however the two zones overlapped at only 4.5% of the forested area.

Not surprisingly, the area where NDVI had the steepest decrease during the 2005–2011 drought was associated with increased dead tree incidence in 2012. For example, average dead tree density was 40.6 trees/ha within the area where $\Delta NDVI_{second} < -0.1$, compared to 7.6 trees/ha within the area where $\Delta NDVI_{second} \geq -0.1$.

NDVI spatiotemporal clusters

Four clusters of NDVI spatiotemporal data occupied distinct geographical areas within the forest (Fig. 7a). However, differences in the NDVI trajectories among clusters could be only partially elucidated by differences in the physical and biotic characteristics of the areas they occupy.
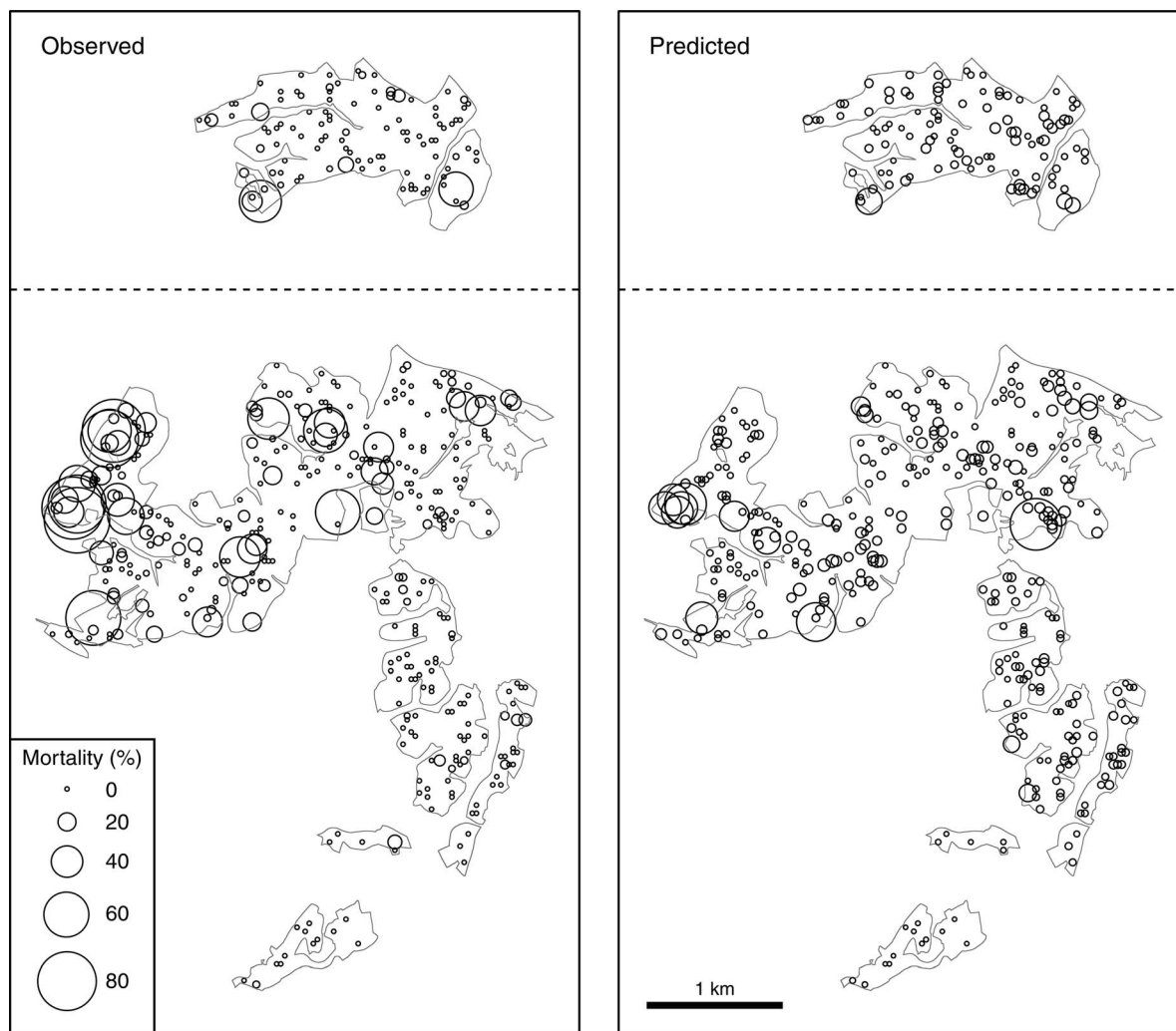
FIG. 5.   Observed proportion of dead trees in Lahav and Dvira forests, and predictions based on a Generalized Linear Model (GLM; Appendix D: Table D1), in 471 randomly placed sample points.

Clusters 1–3 were characterized by NDVI decline with time (Fig. 7b) and had a similar distribution of stand ages and topographic aspects (Appendix F: Table F1). However, they differed in contemporary tree density, in deep soil occurrence, and in mortality percentages (Appendix F: Table F1), as well as in their responses to the first and second droughts (Fig. 7b). Cluster 4 occupied a relatively small part of the forest and consisted of relatively young forest stands (Appendix F: Table F1). It was distinct in the most pronounced way from clusters 1–3 (Fig. 7c), by its increasing trend of NDVI (Fig. 7b) and by its very low mortality (Appendix F: Table F1).

Cluster 1 encompassed the area most severely affected by the recent drought of 2005–2011, with average mortality of 12% (compared to ~3% in clusters 2 and 3; Appendix F: Table F1). Moreover, only cluster 1 included locations with extremely high mortality (60–90%; Fig. 5). Its area also had the lowest average NDVI

by the end of the 2005–2011 drought (Fig. 7b), and the highest proportion of cultivated areas among clusters 1–3 (Appendix F: Table F1). Cluster 2 was the least affected by either the first or second droughts, and had the highest average NDVI in 2011. Cluster 3 was the most severely affected by the 1998–2000 drought, according to the steep NDVI decline (Figs. 6 and 7b). Afterwards, NDVI in cluster 3 was relatively low and stable. Accordingly, current (2012) tree density in this cluster was lowest (Appendix F: Table F1), and included patches with very sparse tree cover.

Tree growth

The responses of tree growth to the first and second droughts according to BAI were in agreement with their responses according to NDVI (Fig. 8). Very low BAI and NDVI values were reached in 2011 in site 1 (1.17 and 0.23 cm/yr, respectively); this site also had the steepest NDVI decline during the 2005–2011 drought
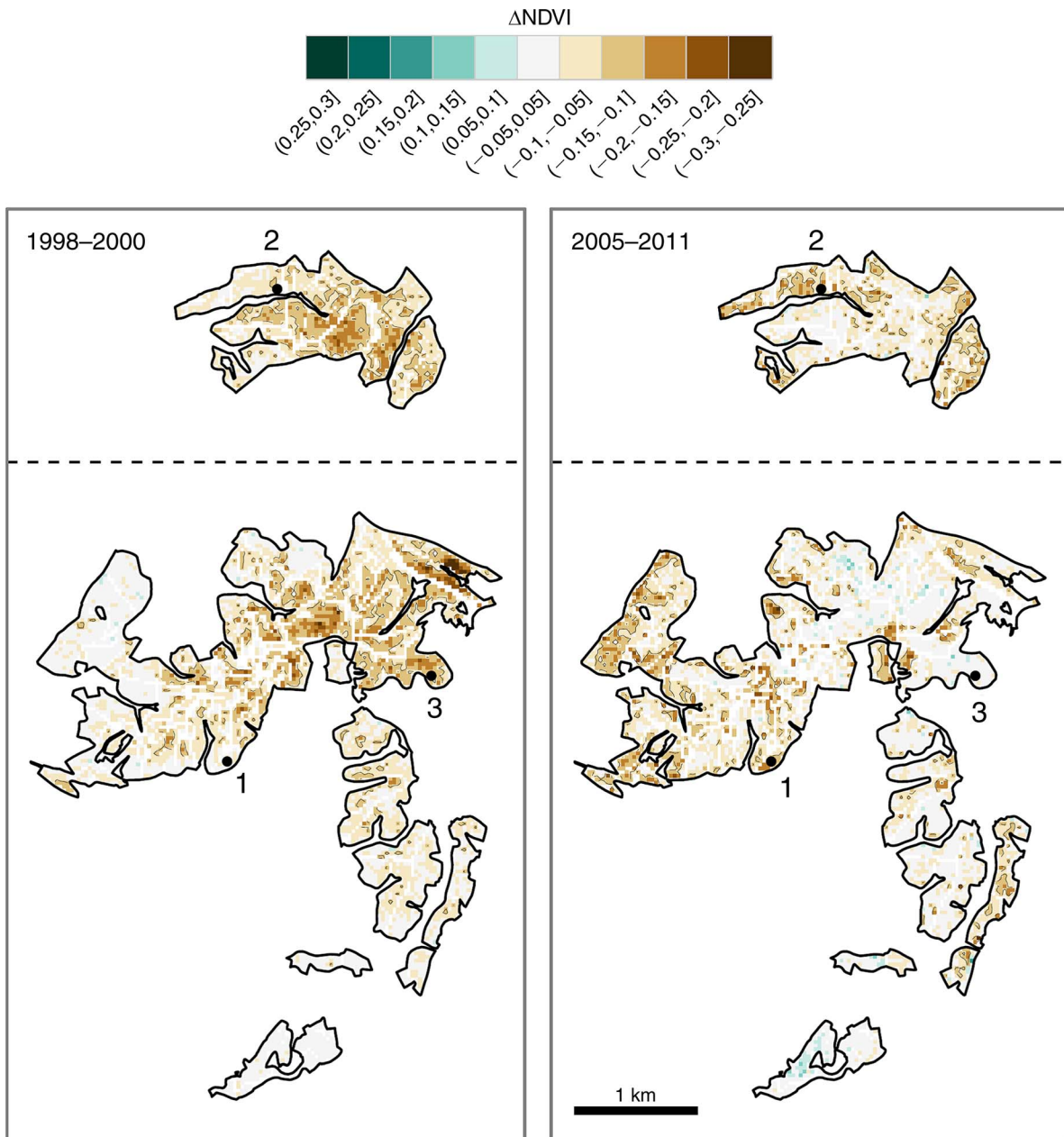
Fig. 6. NDVI (Normalized Difference Vegetation Index) difference between the beginning and the end of the first (1998–2000) and second (2005–2011) drought periods. Areas of ΔNDVI < −0.1 are marked by contours. Sites where dendrochronological sampling was conducted are marked by numbered (1–3) black dots.

(ΔNDVI = −0.16), and substantial mortality (25%) in 2012. Sites 2 and 3 had very little recent mortality (1% and 2%), less steep NDVI declines during the 2005–2011 drought (ΔNDVI = −0.12 and −0.01) and higher BAI (1.77 and 5.29 cm/yr) and NDVI (0.32 and 0.34, respectively) in 2011. According to both BAI and NDVI, the effect of the first drought was strongest in site 3, while the effect of the second drought was strongest in site 1, which is in accordance with the responses of the respective clusters the sites belong to

(Fig. 7b). Tree densities in the three sites (Appendix C) were also representative of the densities in the three respective clusters (Appendix F: Table F1), as site 3 had the lowest density (311.7 trees/ha), compared with sites 1 (373.0 trees/ha) and 2 (527.2 trees/ha).

Tree growth in all three sites closely followed annual rainfall amount; NDVI, however, was associated with rainfall to a lower and less consistent degree (Fig. 8). In site 1, substantial discrepancy between observed and predicted NDVI was reached by 2012, likely as a result
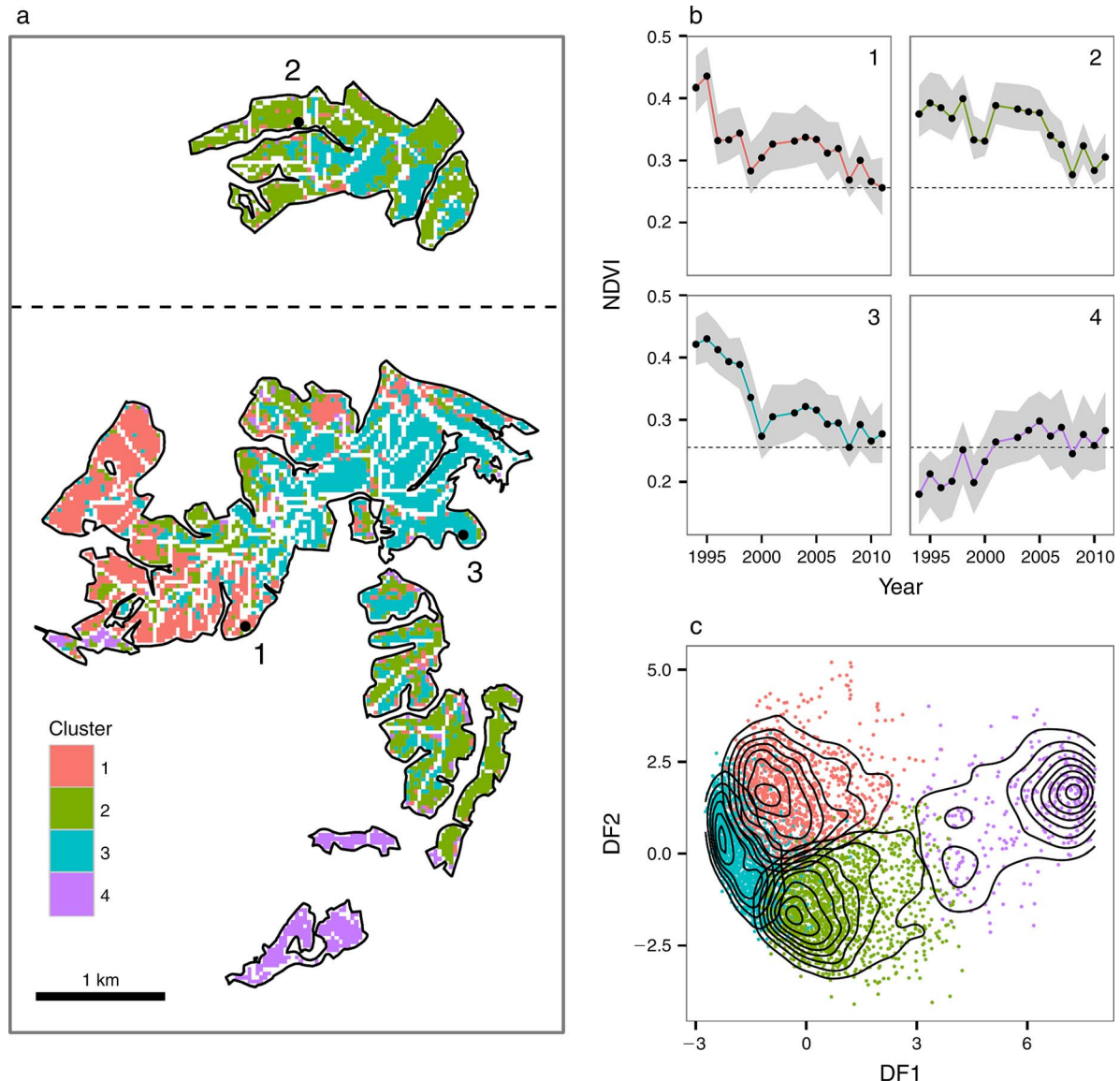
FIG. 7. Spatiotemporal cluster analysis of NDVI (Normalized Difference Vegetation Index) trajectories during 17 years between 1994 and 2011. (a) Locations of the four clusters. Sites where dendrochronological sampling took place are marked by numbered (1–3) black dots. (b) Average and 25–75% inter-quantile range of NDVI values for each cluster, as function of year. The average NDVI value in cluster 1 in 2011 is marked by a dotted line for easier comparison among panels. (c) Separation of observations in the space of the first two discriminant functions (DF1 and DF2). Contours express point density.

of the recent density reduction due to mortality. In site 3, an analogous pattern was observed for the 1998–2000 drought, i.e., a steep NDVI decline (characteristic of the "cluster 3" area, see *Results: NDVI spatiotemporal clusters*) resulting in higher than expected NDVI before 1998 and lower than expected NDVI after 2000 (Fig. 8).

DISCUSSION

Environmental effects on drought-induced mortality

This study has revealed some of the factors associated with increased probability of mortality in semiarid *P. halepensis* forests. Higher mortality was observed in

older stands and on south-facing aspects, which can be expected based on the effects of these factors on soil water availability. Older stands are composed of larger trees, which were frequently found to have higher mortality rates during drought (Floyd et al. 2009, Clifford et al. 2011). For example, mortality of *Pinus edulis* following the 1996 and 2002 severe droughts in Arizona was 2–6 fold higher for larger than smaller tree size classes (Mueller et al. 2005). Higher demands for soil water, and lower vigor due to tissue and cell senescence (Carrer and Urbinati 2004, Peñuelas 2005), may be hypothesized to increase the vulnerability of
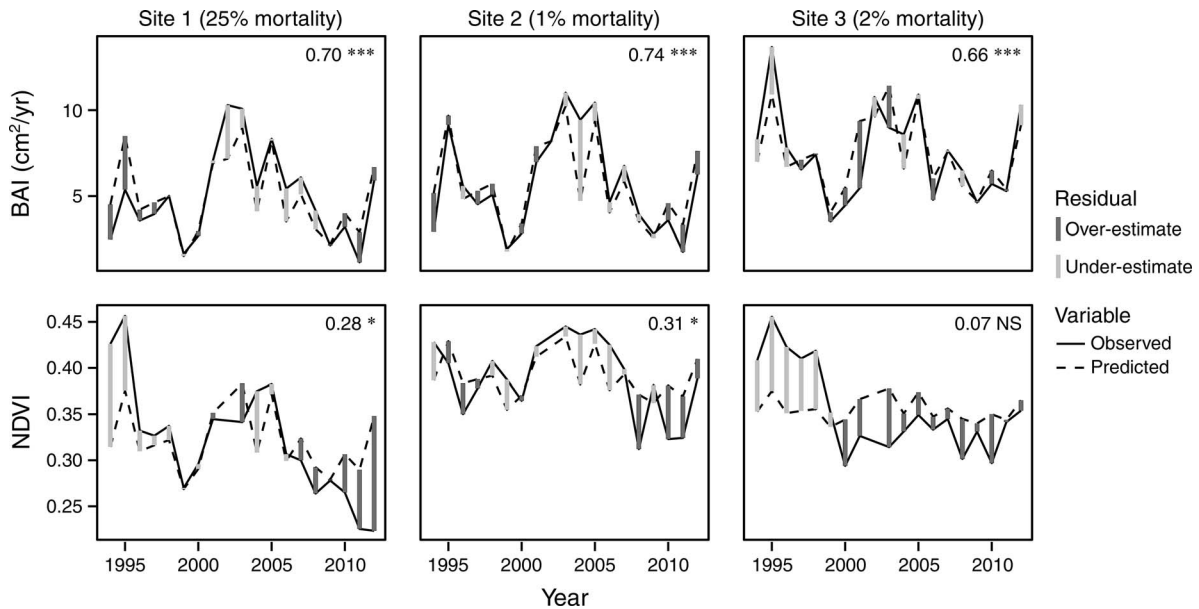
FIG. 8. Observed and predicted Basal Area Increment (BAI) and NDVI for three sites in Lahav and Dvira forests, during the period 1994–2012 (note that NDVI data were not available for 2002). Observed values (solid lines) are averages based on 28, 27, and 30 trees for BAI, and 10, 7, and 10 pixels of 30×30 m^2 for NDVI, in sites 1, 2, and 3, respectively. The numbers in each panel denote R^2 values and significance from linear regressions of the given variable as a function of annual rainfall (* $P < 0.05$, *** $P < 0.001$, NS is not significant). Residuals from the respective models predictions (dashed lines) are shown as dark gray (overestimate) or light gray (underestimate) vertical lines.

older forest trees to drought-induced mortality (Mueller et al. 2005, Floyd et al. 2009, Linares et al. 2013).

South-facing aspects, on the other hand, receiving higher amounts of solar radiation, are subject to higher evaporative demands from the forest canopy, soil, and understory (Pigott and Pigott 1993), resulting in higher drought stress imposed on the forest trees (Huang and Anderegg 2012). Therefore, forest stands on south-facing aspects are most likely to have lower "safety margins" in terms of soil water availability, and they are indeed the first to be affected when drought occurs. The latter is true unless the trees can reduce their dependence on surface moisture by utilizing any existing deeper ground moisture pools (Sarris et al. 2007, 2013). In our case this does not appear to occur, as very high evaporation and limited rainfall may not allow deeper ground moisture pools to form at all (or cause them to become depleted very fast in case they do form during wet years and/or where soil and bedrock types permit).

The higher mortality on deeper soils quantitatively confirms previous qualitative field observations in the region (Y. Moshe, *personal observation*), while higher mortality in sparser stands was unexpected. Both results, however, are seemingly not in agreement with the prevailing view regarding the water supply–demand balance. Deeper soil should contribute to increased water supply (since soil water-holding capacity is higher), while lower tree density should theoretically decrease water demand (since soil water is divided among fewer individuals). We argue that these results

may be in fact characteristic to semiarid regions experiencing extreme drought, where the expectations of density-dependent mortality (e.g., Klos et al. 2009) on shallower soils (e.g., Brouwers et al. 2013a) may not always hold.

A widely advocated strategy for minimizing forest drought vulnerability is tree density reduction (via silvicultural thinning), in order to increase resource availability to the remaining trees within a given population (D'Amato et al. 2013, Ungar et al. 2013). Indeed, increased radial growth rates in response to thinning were consistently observed (e.g., in *P. halepensis* [Olivar et al. 2014], *Pinus ponderosa* [McDowell et al. 2006], and *Abies pinsapo* [Linares et al. 2009b]). Therefore, an association of higher mortality with higher tree density is anticipated due to presumably increased competition intensity in dense locations (Linares et al. 2010, Kerhoulas et al. 2013, Sánchez-Salguero et al. 2013). However, the latter was not steadily observed within the context of widespread forest mortality following extremely dry conditions. For example, associations of higher mortality with *lower* tree densities were observed for *P. edulis* in New Mexico (Clifford et al. 2013) and adjacent areas (Floyd et al. 2009), and for *Populus tremuloides* in Colorado (Worrall et al. 2008); no associations between mortality and density were found for *P. edulis* (Mueller et al. 2005, Clifford et al. 2011) and for mixed-conifer and *P. ponderosa* forests (Ganey and Vojta 2011) in Arizona.

Based on these patterns, it has been suggested that density dependence may be masked under prolonged and extremely limiting drought conditions, leading to mortality across all density levels (Floyd et al. 2009, Ganey and Vojta 2011), while density-dependent mortality is expressed during initial phases of a given drought event (Negron and Wilson 2003). Analogously, the latter "masking" of density-dependent processes has been suggested to vary in space, due to an interaction of density with habitat type (Bowker et al. 2012) or quality (Dwyer et al. 2010). Undoubtedly further studies are necessary to understand the environmental causes for the apparent spatial nonstationary nature of density effect on forest mortality from drought.

Deeper soils, having increased water-holding capacity, were associated with lower mortality following drought in most previous studies (Peterman et al. 2013, Vila-Cabrera et al. 2013), contrary to the present results. However, no association between soil depth and mortality risk was observed in some cases (Brouwers et al. 2013b, Clifford et al. 2013), suggesting that soil depth effect may interact with other factors. A previous study suggested that the threshold for *P. halepensis* survival during drought is determined by the duration of the period between transpirable soil water content exhaustion and the onset of the next-season first rainfalls (Klein et al. 2014). Therefore the key to the survival of this species during extreme drought may involve maintenance of minimal transpirable soil water content during the dry season, rather than overall water-holding capacity.

In water-limited ecosystems, trees roots can penetrate the rock substrate through preferential lines, and rely on the moisture retained in rock fissures when the soil profile dries out (Herr 2008, Schwinning 2010). Access to porous bedrock types such as chalk (Schiller 1982) or to limited-infiltration soil layers (Klein et al. 2014) may therefore provide an important source of slowly depleting moisture reserves at times of drought for trees growing on shallow soils (Schiller et al. 2002, 2010, Breshears et al. 2009a, Sarris et al. 2013). Deep soils, although beneficial during normal climatic conditions due to higher water-holding capacity, may impose "hydraulic overextension" (Ogle et al. 2000, Fensham and Fairfax 2007, Allen et al. 2010), e.g., through development of a relatively shallow root system (Bellot et al. 2004, Klein et al. 2014). In addition, pines in southern Israel were found to depend on annual (mostly winter) rainfall for growth vs. multiple years of past rainfall determining growth in more humid conditions to the north (Dorman et al., *in press*). This finding suggests that shallow-rooted trees dominate within the southernmost pine populations. The combination of a shallow root system and deep soil could lead to elevated vulnerability in times of drought, when the entire soil profile dries out, while water stored in rock layers is beyond the reach of tree roots (Fensham and Fairfax 2007). We would expect the latter effect to be strongest where evapotranspiration demand is highest, for example on southern aspects (Schiller et al. 2009), as indeed has been observed in the present study (Fig. 4).

Patchy, spatially variable, density-independent mortality; possible causes

The fine-grained spatial pattern of mortality was patchy at the whole range of relevant spatial scales; consequently the exact magnitude of mortality was largely unpredictable ($R^2 = 0.23$) to a similar degree compared with previous studies. For example, Clifford et al. (2013) could explain 14% of the spatial variation in *P. edulis* mortality in New Mexico (USA), following an extreme drought in 2002–2003 (Weiss et al. 2009); Brouwers et al. (2013a) could explain 15% of canopy dieback in southwestern Australia mediterranean forests, following an extreme drought in 2010–2011.

In some of the previous studies a division could be made between what were a posteriori identified as "high-risk" zones, where both low and high mortality levels were observed (e.g., elevation <1300 m [Linares et al. 2009a]; 2-year rainfall sum <600 mm [Clifford et al. 2013]; lower average rainfall combined with proximity to rock outcrops [Brouwers et al. 2013a, Matusick et al. 2013]; previously cultivated areas on southern aspects [present study]), in contrast to "low-risk" zones, where mortality was uniformly low. In others, no such division was apparent (Ganey and Vojta 2011). These results translate to considerable uncertainty in forecasting when and where forest mortality would occur within the landscape in future drought events, which greatly constrains management options (Breshears et al. 2011, López-Hoffman et al. 2013; see *Discussion: Implications to forest resilience following drought*).

By exploring two sequential droughts using remote sensing and dendrochronological measurements, our study further demonstrates the complexity of mortality dynamics. Not only was the spatial pattern of forest decline largely unpredicted by environmental conditions; two different parts of the forest were affected during the two drought periods (but see Mueller et al. 2005, where the opposite pattern, repeated mortality in the same locations, was observed).

Two main types of explanation, which are not mutually exclusive, may be offered for the apparently spatially autocorrelated random component in mortality. *First*, a key environmental factor (or factors), which is itself spatially autocorrelated, could be missing in the analysis (Zuur et al. 2009:177–182), thus indirectly leading to spatial "attraction" of tree mortality events. For instance, soil micro-topography (Querejeta et al. 2001, Zaady et al. 2001, Saquete Ferrandiz et al. 2006), its depth and composition (Schiller 1972, Olarieta et al. 2000), profile structure (Schiller 1977, Klein et al. 2014), and underlying lithology (Schiller 1982, Weinstein-Evron and Lev-Yadun 2000) have all been previously shown to affect development of *P. halepensis*. Since it

would be difficult to map such properties at a high resolution for extensive areas, understanding their role in forest decline from drought currently remains restricted to field sites covering limited spatial extents. However, the difference in spatial locations of affected areas in the two droughts (Fig. 6) does not support the hypothesis that the remaining variation in forest decline is exclusively related to substrate properties. If that was the case, we would expect the same locations to be affected in both drought periods, since substrate structure remains invariable within the studied time frame.

Local-scale spatial variation in rainfall amounts may also account for differences in degree of drought stress among different locations within the forest. This may be especially relevant in semiarid regions, where the limiting effect of rainfall on vegetation is relatively strong (i.e., even small changes in rainfall amount may generate large differences in forest performance [Fritts et al. 1965]), while the local-scale spatial variability in rainfall amount is relatively high (i.e., nearby locations within the landscape may receive different amounts of rainfall [Syed et al. 2003, Yakir and Morin 2011]). Finally, since the planted forests were established from foreign seed sources of undocumented origin (Schiller 2013), the potential role of adaptation to arid conditions of different genetic backgrounds (Schiller and Atzmon 2009) cannot be ruled out as an additional source of mortality variation.

Second, dead trees may elevate the mortality risk in their surroundings, so that randomly scattered initiation points expand into mortality patches by self-amplifying dynamics (Peters et al. 2004), resulting in an auto-correlated pattern. At least two mechanisms may account for such a pattern: increasing pathogens load and modification of the physical environment by dead trees. As for the first mechanism, dead or dying trees could, for example, negatively affect their proximate environment by serving as suitable hosts for diseases and parasites, thus facilitating attack on healthy trees, thereby driving a local outbreak (Allen 2007, Liu et al. 2007, Raffa et al. 2008). As for the second mechanism, the increasing water availability due to mortality may be counterbalanced, or even surpassed, by increased soil water loss due to the proliferation of herbaceous vegetation and greater solar radiation load (Rich et al. 2008, Kane et al. 2011). In other words, greater canopy openness is accompanied by increased near-ground solar radiation and associated soil temperature (Breshears et al. 1998, Royer et al. 2011), which may increase evapotranspiration from soil and understory vegetation, posing additional stress on the remaining trees. For example, in a previous study where soil evaporation in a planted *P. halepensis* forest from the semiarid region has been measured in shaded and sun-exposed areas, evaporation was found to be double, on average, in the latter (Raz-Yaseef et al. 2010).

Implications to forest resilience following drought

A previous study (Dorman et al., *in press*) has shown that, at the individual tree level, the effect of competition on tree growth in the planted *P. halepensis* forests follows a heterogeneous pattern across portions of the population having different growth rates. Specifically, while in the relatively slow-growing trees BAI was not associated with competition intensity, in the relatively fast-growing trees BAI was significantly (negatively) affected by competition. Since slow growth is associated with elevated mortality risk, it was hypothesized that mortality was not associated with higher densities. This hypothesis was supported by the present study. In other words, slow-growing individual trees (Dorman et al., *in press*) and locations of elevated mortality risk (the present study) were *not* more likely to be found under high competition intensities. Moreover, the association of higher mortality risk with *lower* tree density, and the spatially aggregated mortality pattern, imply that the performance of individual trees was not improved no matter how much competition pressure was reduced. From the point of view of forest management, we hypothesize that thinning may further improve tree growth at improved habitats, but it may not "save" predisposed stands experiencing extreme drought where patches of high (up to almost complete) mortality are initiated at unpredictable locations.

The very high agreement between BAI and annual rainfall in the semiarid forests (Fig. 8) expresses the low resistance, but high resilience, that individual *P. halepensis* trees may exhibit when facing drought. For example, the surviving trees in all three sites have quickly recovered their "usual" growth rates in 2012, following the 2005–2011 drought, even in site 1 where 25% mortality was observed. However, in order to generalize about resistance and resilience properties from individual trees to the forest ecosystem as a whole, it is essential to evaluate forest demographic trends as well (Lloret et al. 2011). Demographic information may be available from tree ring data alone (although for limited spatial extents), in cases when dead trees remain on site in datable condition (e.g., Suarez et al. 2004, Bigler et al. 2007). Otherwise, taking into account only living (surviving) trees may result in underestimation of resilience in drought-affected areas (Breda and Badeau 2008). Moreover, there is often no way of knowing the degree of removal and/or decay of wood material that took place in a given site for several decades into the past, and thus the degree of bias. Since satellite images are obtained in real time, rather than in retrospect, they may provide valuable reference information in such cases. For example, the tree density reduction in site 1, due to mortality following the 2005–2011 drought, was reflected by the lack of NDVI recovery during the relatively wet year of 2012 (Fig. 8). Similarly, the density reduction in site 3 during the 1998–2000 drought, likely due to drought-induced mortality, was indicated by the permanent NDVI decline in that time period (Fig. 8).

Substantial mortality has been observed in 2012 in the present study, and similar observations were made in the other forests of the southern region, by means of remote sensing (Dorman et al. 2013b) and field observations (local foresters, *personal communication*). Nevertheless, the systematic mapping of mortality rates has revealed that mortality was extremely low for large parts of the forests, even though the forests are located beyond the natural distribution area of the species. Thus even under such extreme climatic conditions, *P. halepensis* seems to have the potential to survive severe drought events.

Conclusions

The semiarid planted *P. halepensis* forests that we studied have recently (2005–2011) experienced the most severe drought in at least ~50 years (Fig. 2). The degree and spatial pattern of drought-induced damage were evaluated, for the first time to the best of our knowledge, simultaneously on three distinct levels of organizational complexity. The following main conclusions, directly related to forest management applications under climatic change, may change the way we think about monitoring and management of arid forest borders.

First, the association of mortality with lower tree densities does not support the notion that thinning semiarid forests will necessarily increase survival probability of the remaining trees (Ganey and Vojta 2011). Accordingly, the benefits of thinning, currently considered the main forest management tool to enhance resistance to drought (e.g., Linares et al. 2010, Vila-Cabrera et al. 2011, Ungar et al. 2013), are questionable and require further research, at least within the context of extreme drought events in semiarid ecosystems.

Second, mortality was spatially clustered, and its magnitude was largely unexplained by the physical and biotic environmental factors that can be feasibly mapped for large continuous areas. The fact that patches of substantial (up to 90%) forest cover loss may show up, apparently unpredictably, within "higher-risk" zones (e.g., older age, south-facing slopes) should be acknowledged by forest managers, especially in semiarid forests where enhanced survival probability (and not, for example, timber yield) is defined as the main management objective.

Third, it was demonstrated that the multi-perspective approach provides a more complete understanding of the studied phenomenon. While inferences based on the different methods were generally in agreement, the differences were informatively related to the different levels of organization each method addresses, making them complementary (Levin 1992). For example, dendrochronological methods account only for the portion of population present at the time of sampling, thus potentially overestimating forest resilience, while satellite remote sensing may aggregate the reflectance of large forest canopy "portions," thus limiting the attribution of decline to either demographic (e.g., mortality) or structural (e.g., defoliation) processes (Macfarlane et al. 2013). We therefore suggest that evaluation of forest ecosystems resilience should ultimately be based on an integration of several metrics, each suited for detecting transitions at a different level of organization, from individual trees performance (e.g., BAI), to short-term demographic trends (e.g., mortality rates) and ultimately to long-term changes in forest ecosystem functioning (e.g., remotely sensed vegetation indices).

Literature Cited

Akaike, H. 1974. A new look at the statistical model identification. IEEE Transactions on Automatic Control AC19:716–723.

Allen, C. D. 2007. Interactions across spatial scales among forest dieback, fire, and erosion in northern New Mexico landscapes. Ecosystems 10:797–808.

Allen, C. D., and D. D. Breshears. 1998. Drought-induced shift of a forest-woodland ecotone: rapid landscape response to climate variation. Proceedings of the National Academy of Sciences USA 95:14839–14842.

Allen, C. D., et al. 2010. A global overview of drought and heat-induced tree mortality reveals emerging climate change risks for forests. Forest Ecology and Management 259:660–684.

Anderegg, W. R. L., J. A. Berry, D. D. Smith, J. S. Sperry, L. D. L. Anderegg, and C. B. Field. 2012. The roles of hydraulic and carbon stress in a widespread climate-induced forest die-off. Proceedings of the National Academy of Sciences USA 109:233–237.

Anderegg, W. R. L., J. M. Kane, and L. D. L. Anderegg. 2013a. Consequences of widespread tree mortality triggered by drought and temperature stress. Nature Climate Change 3:30–36.

Anderegg, W. R. L., L. Plavcova, L. D. L. Anderegg, U. G. Hacke, J. A. Berry, and C. B. Field. 2013b. Drought's legacy: multiyear hydraulic deterioration underlies widespread aspen forest die-off and portends increased future risk. Global Change Biology 19:1188–1196.

Anderson, L. O., Y. Malhi, L. E. O. C. Aragao, R. Ladle, E. Arai, N. Barbier, and O. Phillips. 2010. Remote sensing detection of droughts in Amazonian forest canopies. New Phytologist 187:733–750.

Babst, F., J. Esper, and E. Parlow. 2010. Landsat TM/ETM plus and tree-ring based assessment of spatiotemporal patterns of the autumnal moth (*Epirrita autumnata*) in northernmost Fennoscandia. Remote Sensing of Environment 114:637–646.

Baddeley, A., and R. Turner. 2005. spatstat: an R package for analyzing spatial point patterns. Journal of Statistical Software 12:1–42.

Baguskas, S. A., S. H. Peterson, B. Bookhagen, and C. J. Still. 2014. Evaluating spatial patterns of drought-induced tree mortality in a coastal California pine forest. Forest Ecology and Management 315:43–53.

Beck, P. S. A., G. P. Juday, C. Alix, V. A. Barber, S. E. Winslow, E. E. Sousa, P. Heiser, J. D. Herriges, and S. J. Goetz. 2011. Changes in forest productivity across Alaska consistent with biome shift. Ecology Letters 14:373–379.

Bellot, J., F. T. Maestre, E. Chirino, N. Hernández, and J. O. de Urbina. 2004. Afforestation with *Pinus halepensis* reduces native shrub performance in a Mediterranean semiarid area. Acta Oecologica 25:7–15.

Berner, L. T., P. S. A. Beck, A. G. Bunn, A. H. Lloyd, and S. J. Goetz. 2011. High-latitude tree growth and satellite vegetation indices: correlations and trends in Russia and Canada (1982–2008). Journal of Geophysical Research-Biogeosciences 116(G1). G01015. http://dx.doi.org/10.1029/2010JG001475

Bigler, C., D. G. Gavin, C. Gunning, and T. T. Veblen. 2007. Drought induces lagged tree mortality in a subalpine forest in the Rocky Mountains. Oikos 116:1983–1994.

Biondi, F., and F. Qeadan. 2008. A theory-driven approach to tree-ring standardization: defining the biological trend from expected basal area increment. Tree-Ring Research 64:81–96.

Bivand, R. S., E. J. Pebesma, and V. Gomez-Rubio. 2008. Applied spatial data analysis with R. Springer, New York, New York, USA.

Bowker, M. A., A. Muñoz, T. Martinez, and M. K. Lau. 2012. Rare drought-induced mortality of juniper is enhanced by edaphic stressors and influenced by stand density. Journal of Arid Environments 76:9–16.

Breda, N., and V. Badeau. 2008. Forest tree responses to extreme drought and some biotic events: towards a selection according to hazard tolerance? Comptes Rendus Geoscience 340:651–662.

Breshears, D. D., L. Lopez-Hoffman, and L. J. Graumlich. 2011. When ecosystem services crash: preparing for big, fast, patchy climate change. Ambio 40:256–263.

Breshears, D. D., O. B. Myers, and F. J. Barnes. 2009a. Horizontal heterogeneity in the frequency of plant-available water with woodland intercanopy-canopy vegetation patch type rivals that occuring vertically by soil depth. Ecohydrology 2:503–519.

Breshears, D. D., O. B. Myers, C. W. Meyer, F. J. Barnes, C. B. Zou, C. D. Allen, N. G. McDowell, and W. T. Pockman. 2009b. Tree die-off in response to global change-type drought: mortality insights from a decade of plant water potential measurements. Frontiers in Ecology and the Environment 7:185–189.

Breshears, D. D., J. W. Nyhan, C. E. Heil, and B. P. Wilcox. 1998. Effects of woody plants on microclimate in a semiarid woodland: Soil temperature and evaporation in canopy and intercanopy patches. International Journal of Plant Sciences 159:1010–1017.

Brouwers, N., G. Matusick, K. Ruthrof, T. Lyons, and G. Hardy. 2013a. Landscape-scale assessment of tree crown dieback following extreme drought and heat in a Mediterranean eucalypt forest ecosystem. Landscape Ecology 28:69–80.

Brouwers, N. C., J. Mercer, T. Lyons, P. Poot, E. Veneklaas, and G. Hardy. 2013b. Climate and landscape drivers of tree decline in a Mediterranean ecoregion. Ecology and Evolution 3:67–79.

Carrer, M., and C. Urbinati. 2004. Age-dependent tree-ring growth responses to climate in *Larix decidua* and *Pinus cembra.* Ecology 85:730–740.

Chapman, T. B., T. T. Veblen, and T. Schoennagel. 2012. Spatiotemporal patterns of mountain pine beetle activity in the southern Rocky Mountains. Ecology 93:2175–2185.

Chen, J., X. Zhu, J. E. Vogelmann, F. Gao, and S. Jin. 2011. A simple and effective method for filling gaps in Landsat ETM+ SLC-off images. Remote Sensing of Environment 115:1053–1064.

Clifford, M. J., N. S. Cobb, and M. Buenemann. 2011. Long-term tree cover dynamics in a pinyon-juniper woodland: climate-change-type drought resets successional clock. Ecosystems 14:949–962.

Clifford, M. J., P. D. Royer, N. S. Cobb, D. D. Breshears, and P. L. Ford. 2013. Precipitation thresholds and drought-induced tree die-off: insights from patterns of *Pinus edulis* mortality along an environmental stress gradient. New Phytologist 200:413–421.

D'Amato, A. W., J. B. Bradford, S. Fraver, and B. J. Palik. 2013. Effects of thinning on drought vulnerability and climate response in north temperate forest ecosystems. Ecological Applications 23:1735–1742.

Dan, J., D. H. Yaalon, H. Koyumdjisky, and Z. Raz. 1970. The soil association map of Israel. Pamphlet-Agricultural Research Organization, (Israel). Israel Journal of Earth-Sciences 21:29–49.

de Luis, M., K. Čufar, A. Di Filippo, K. Novak, A. Papadopoulos, G. Piovesan, C. B. K. Rathgeber, J. Raventós, M. A. Saz, and K. T. Smith. 2013. Plasticity in dendroclimatic response across the distribution range of Aleppo pine (*Pinus halepensis*). PLoS ONE 8:e83550.

Dorman, M., A. Perevolotsky, D. Sarris, and T. Svoray. The effect of rainfall and competition intensity on forest response to drought: lessons learned from a dry extreme. Oecologia, *in press.*

Dorman, M., T. Svoray, and A. Perevolotsky. 2012. Tree mortality in *Pinus halepensis* forests of Israel:a remote sensing approach. [In Hebrew.] Ecology and Environment 3:230–237.

Dorman, M., T. Svoray, and A. Perevolotsky. 2013a. Homogenization in forest performance across an environmental gradient: the interplay between rainfall and topographic aspect. Forest Ecology and Management 310:256–266.

Dorman, M., T. Svoray, A. Perevolotsky, and D. Sarris. 2013b. Forest performance during two consecutive drought periods: diverging long-term trends and short-term responses along a climatic gradient. Forest Ecology and Management 310:1–9.

Dwyer, J. M., R. J. Fensham, R. J. Fairfax, and Y. M. Buckley. 2010. Neighbourhood effects influence drought-induced mortality of savanna trees in Australia. Journal of Vegetation Science 21:573–585.

Fensham, R. J., and R. J. Fairfax. 2007. Drought-related tree death of savanna eucalypts: species susceptibility, soil conditions and root architecture. Journal of Vegetation Science 18:71–80.

Fensham, R. J., R. J. Fairfax, and S. R. Archer. 2005. Rainfall, land use and woody vegetation cover change in semi-arid Australian savanna. Journal of Ecology 93:596–606.

Floyd, M. L., M. Clifford, N. S. Cobb, D. Hanna, R. Delph, P. Ford, and D. Turner. 2009. Relationship of stand characteristics to drought-induced mortality in three Southwestern pinon–juniper woodlands. Ecological Applications 19:1223–1230.

Fortin, M. J., and M. R. T. Dale. 2005. Spatial analysis: a guide for ecologists. Cambridge University Press, Cambridge, UK.

Fritts, H. C., D. G. Smith, J. W. Cardis, and C. A. Budelsky. 1965. Tree-ring characteristics along a vegetation gradient in northern Arizona. Ecology 46:393–401.

Fu, P. D., and P. M. Rich. 2002. A geometric solar radiation model with applications in agriculture and forestry. Computers and Electronics in Agriculture 37:25–35.

Galiano, L., J. Martinez-Vilalta, and F. Lloret. 2011. Carbon reserves and canopy defoliation determine the recovery of Scots pine 4 yr after a drought episode. New Phytologist 190:750–759.

Ganey, J. L., and S. C. Vojta. 2011. Tree mortality in drought-stressed mixed-conifer and ponderosa pine forests, Arizona, USA. Forest Ecology and Management 261:162–168.

Garrity, S. R., C. D. Allen, S. P. Brumby, C. Gangodagamage, N. G. McDowell, and D. M. Cai. 2013. Quantifying tree mortality in a mixed species woodland using multitemporal high spatial resolution satellite imagery. Remote Sensing of Environment 129:54–65.

Girard, F., M. Vennetier, F. Guibal, C. Corona, S. Ouarmim, and A. Herrero. 2012. *Pinus halepensis* Mill. crown development and fruiting declined with repeated drought in Mediterranean France. European Journal of Forest Research 131:919–931.

Girard, F., M. Vennetier, S. Ouarmim, Y. Caraglio, and L. Misson. 2011. Polyclism, a fundamental tree growth process, decline with recent climate change: the example of *Pinus halepensis* Mill. in Mediterranean France. Trees-Structure and Function 25:311–322.

Gitlin, A. R., C. M. Sthultz, M. A. Bowker, S. Stumpf, K. L. Paxton, K. Kennedy, A. Munoz, J. K. Bailey, and T. G. Whitham. 2006. Mortality gradients within and among dominant plant populations as barometers of ecosystem change during extreme drought. Conservation Biology 20:1477–1486.

Goslee, S. C. 2011. Analyzing remote sensing data in R: The landsat package. Journal of Statistical Software 43:1–25.

Hall, J. K., and R. L. Cleave. 1988. The DTM project. Geological Survey of Israel 6:1–7.

Hargreaves, G. H. 1994. Defining and using reference evapotranspiration. Journal of Irrigation and Drainage Engineering-ASCE 120:1132–1139.

Hartigan, J. A., and M. A. Wong. 1979. A K-means clustering algorithm. Applied Statistics 28:100–108.

Herr, N. 2008. Rock-soil system and water regime dynamics in the habitat as the main ecological factors of *Quercus ithaburensis* and *Quercus calliprinos* in Alonim-Menashe region. Dissertation. Hebrew University of Jerusalem, Jerusalem, Israel.

Hicke, J. A., and M. J. B. Zeppel. 2013. Climate-driven tree mortality: insights from the piñon pine die-off in the United States. New Phytologist 200:301–303.

Hothorn, T., and B. S. Everitt. 2009. A handbook of statistical analyses using R. Second edition. Taylor and Francis, London, UK.

Huang, C.-Y., and W. R. L. Anderegg. 2012. Large drought-induced aboveground live biomass losses in southern Rocky Mountain aspen forests. Global Change Biology 18:1016–1027.

Johnson, J. B., and K. S. Omland. 2004. Model selection in ecology and evolution. Trends in Ecology and Evolution 19:101–108.

Kane, J. M., K. A. Meinhardt, T. Chang, B. L. Cardall, R. Michalet, and T. G. Whitham. 2011. Drought-induced mortality of a foundation species (*Juniperus monosperma*) promotes positive afterlife effects in understory vegetation. Plant Ecology 212:733–741.

Kerhoulas, L. P., T. E. Kolb, M. D. Hurteau, and G. W. Koch. 2013. Managing climate change adaptation in forests: a case study from the U.S. Southwest. Journal of Applied Ecology 50:1311–1320.

Kharuk, V. I., S. T. Im, P. A. Oskorbin, I. A. Petrov, and K. J. Ranson. 2013. Siberian pine decline and mortality in southern Siberian mountains. Forest Ecology and Management 310:312–320.

Klein, T., E. Rotenberg, E. Cohen-Hilaleh, N. Raz-Yaseef, F. Tatarinov, Y. Preisler, J. Ogée, S. Cohen, and D. Yakir. 2014. Quantifying transpirable soil water and its relations to tree water use dynamics in a water-limited pine forest. Ecohydrology 7:409–419.

Klos, R. J., G. G. Wang, W. L. Bauerle, and J. R. Rieck. 2009. Drought impact on forest growth and mortality in the southeast USA: an analysis using Forest Health and Monitoring data. Ecological Applications 19:699–708.

le Polain de Waroux, Y., and E. F. Lambin. 2012. Monitoring degradation in arid and semi-arid forests and woodlands: the case of the argan woodlands (Morocco). Applied Geography 32:777–786.

Levin, S. A. 1992. The problem of pattern and scale in ecology: the Robert H. MacArthur award lecture. Ecology 73:1943–1967.

Linares, J. C., J. J. Camarero, and J. A. Carreira. 2009a. Interacting effects of changes in climate and forest cover on mortality and growth of the southernmost European fir forests. Global Ecology and Biogeography 18:485–497.

Linares, J. C., J. J. Camarero, and J. A. Carreira. 2009b. Plastic responses of *Abies pinsapo* xylogenesis to drought and competition. Tree Physiology 29:1525–1536.

Linares, J. C., J. J. Camarero, and J. A. Carreira. 2010. Competition modulates the adaptation capacity of forests to climatic stress: insights from recent growth decline and death in relict stands of the Mediterranean fir *Abies pinsapo*. Journal of Ecology 98:592–603.

Linares, J. C., L. Taiqui, G. Sangueesa-Barreda, J. Ignacio Seco, and J. Julio Camarero. 2013. Age-related drought sensitivity of Atlas cedar (*Cedrus atlantica*) in the Moroccan Middle Atlas forests. Dendrochronologia 31:88–96.

Liphschitz, N., and G. Biger. 2001. Past distribution of Aleppo pine (*Pinus halepensis*) in the mountains of Israel (Palestine). Holocene 11:427–436.

Liu, D., M. Kelly, P. Gong, and Q. Guo. 2007. Characterizing spatial–temporal tree mortality patterns associated with a new forest disease. Forest Ecology and Management 253:220–231.

Lloret, F., E. G. Keeling, and A. Sala. 2011. Components of tree resilience: effects of successive low-growth episodes in old ponderosa pine forests. Oikos 120:1909–1920.

Lloyd, A. H., A. G. Bunn, and L. Berner. 2011. A latitudinal gradient in tree growth response to climate warming in the Siberian taiga. Global Change Biology 17:1935–1945.

Lopatin, E., T. Kolstrom, and H. Spiecker. 2006. Determination of forest growth trends in Komi Republic (northwestern Russia): combination of tree-ring analysis and remote sensing data. Boreal Environment Research 11:341–353.

López-Hoffman, L., D. D. Breshears, C. D. Allen, and M. L. Miller. 2013. Key landscape ecology metrics for assessing climate change adaptation options: rate of change and patchiness of impacts. Ecosphere 4:art101.

Macfarlane, W. W., J. A. Logan, and W. R. Kern. 2013. An innovative aerial assessment of Greater Yellowstone Ecosystem mountain pine beetle-caused whitebark pine mortality. Ecological Applications 23:421–437.

Matusick, G., K. X. Ruthrof, N. C. Brouwers, B. Dell, and G. S. J. Hardy. 2013. Sudden forest canopy collapse corresponding with extreme drought and heat in a mediterranean-type eucalypt forest in southwestern Australia. European Journal of Forest Research 132:497–510.

Matyas, C. 2010. Forecasts needed for retreating forests. Nature 464:1271.

McDowell, N. G., H. D. Adams, J. D. Bailey, M. Hess, and T. E. Kolb. 2006. Homeostatic maintenance of ponderosa pine gas exchange in response to stand density changes. Ecological Applications 16:1164–1182.

McDowell, N. G., D. J. Beerling, D. D. Breshears, R. A. Fisher, K. F. Raffa, and M. Stitt. 2011. The interdependence of mechanisms underlying climate-driven vegetation mortality. Trends in Ecology and Evolution 26:523–532.

McDowell, N. G., R. A. Fisher, C. Xu, J. C. Domec, T. Hölttä, D. S. Mackay, J. S. Sperry, A. Boutz, L. Dickman, and N. Gehres. 2013a. Evaluating theories of drought-induced vegetation mortality using a multimodel–experiment framework. New Phytologist 200:304–321.

McDowell, N., W. T. Pockman, C. D. Allen, D. D. Breshears, N. Cobb, T. Kolb, J. Plaut, J. Sperry, A. West, D. G. Williams, and E. A. Yepez. 2008. Mechanisms of plant survival and mortality during drought: why do some plants survive while others succumb to drought? New Phytologist 178:719–739.

McDowell, N. G., M. G. Ryan, M. J. B. Zeppel, and D. T. Tissue. 2013b. Improving our knowledge of drought-induced forest mortality through experiments, observations, and modeling. New Phytologist 200:289–293.

Michaelian, M., E. H. Hogg, R. J. Hall, and E. Arsenault. 2011. Massive mortality of aspen following severe drought along the southern edge of the Canadian boreal forest. Global Change Biology 17:2084–2094.

Mora, C., et al. 2013. The projected timing of climate departure from recent variability. Nature 502:183–187.

Mueller, R. C., C. M. Scudder, M. E. Porter, R. T. Trotter, C. A. Gehring, and T. G. Whitham. 2005. Differential tree mortality in response to severe drought: evidence for long-term vegetation shifts. Journal of Ecology 93:1085–1093.

Negron, J. F., and J. L. Wilson. 2003. Attributes associated with probability of infestation by the pinon ips, *Ips confusus* (Coleoptera: Scolytidae), in pinon pine, *Pinus edulis*. Western North American Naturalist 63:440–451.

Ogle, K., T. G. Whitham, and N. S. Cobb. 2000. Tree-ring variation in pinyon predicts likelihood of death following severe drought. Ecology 81:3237–3243.

Olarieta, J. R., A. Uson, R. Rodriguez, M. Rosa, R. Blanco, and M. Antunez. 2000. Land requirements for *Pinus halepensis* Mill. growth in a plantation in Huesca, Spain. Soil Use and Management 16:88–92.

Olivar, J., S. Bogino, C. Rathgeber, V. Bonnesoeur, and F. Bravo. 2014. Thinning has a positive effect on growth dynamics and growth–climate relationships in Aleppo pine (*Pinus halepensis*) trees of different crown classes. Annals of Forest Science 71:395–404.

Osem, Y., H. Yavlovich, N. Zecharia, N. Atzmon, Y. Moshe, and G. Schiller. 2013. Fire-free natural regeneration in water limited *Pinus halepensis* forests: a silvicultural approach. European Journal of Forest Research 132:679–690.

Osem, Y., E. Zangy, E. Bney-Moshe, Y. Moshe, N. Karni, and Y. Nisan. 2009. The potential of transforming simple structured pine plantations into mixed Mediterranean forests through natural regeneration along a rainfall gradient. Forest Ecology and Management 259:14–23.

Peñuelas, J. 2005. Plant physiology: a big issue for trees. Nature 437:965–966.

Perevolotsky, A., and E. Sheffer. 2009. Forest management in Israel—the ecological alternative. Israel Journal of Plant Sciences 57:35–48.

Peterman, W., R. H. Waring, T. Seager, and W. L. Pollock. 2013. Soil properties affect pinyon pine–juniper response to drought. Ecohydrology 6:455–463.

Peters, D. P. C., R. A. Pielke, B. T. Bestelmeyer, C. D. Allen, S. Munson-McGee, and K. M. Havstad. 2004. Cross-scale interactions, nonlinearities, and forecasting catastrophic events. Proceedings of the National Academy of Sciences USA 101:15130–15135.

Pettorelli, N., J. O. Vik, A. Mysterud, J.-M. Gaillard, C. J. Tucker, and N. C. Stenseth. 2005. Using the satellite-derived NDVI to assess ecological responses to environmental change. Trends in Ecology and Evolution 20:503–510.

Pigott, C. D., and S. Pigott. 1993. Water as a determinant of the distribution of trees at the boundary of the Mediterranean zone. Journal of Ecology 81:557–566.

Plant, R. E. 2012. Spatial data analysis in ecology and agriculture using R. Taylor and Francis, London, UK.

Querejeta, J. I., A. Roldan, J. Albaladejo, and V. Castillo. 2001. Soil water availability improved by site preparation in a *Pinus halepensis* afforestation under semiarid climate. Forest Ecology and Management 149:115–128.

R Development Core Team. 2013. R: A language and environment for statistical computing. R Foundation for Statistical Computing, Vienna, Austria.

Raffa, K. F., B. H. Aukema, B. J. Bentz, A. L. Carroll, J. A. Hicke, M. G. Turner, and W. H. Romme. 2008. Cross-scale drivers of natural disturbances prone to anthropogenic amplification: the dynamics of bark beetle eruptions. BioScience 58:501–517.

Raz-Yaseef, N., E. Rotenberg, and D. Yakir. 2010. Effects of spatial variations in soil evaporation caused by tree shading on water flux partitioning in a semi-arid pine forest. Agricultural and Forest Meteorology 150:454–462.

Raz-Yaseef, N., D. Yakir, G. Schiller, and S. Cohen. 2012. Dynamics of evapotranspiration partitioning in a semi-arid forest as affected by temporal rainfall patterns. Agricultural and Forest Meteorology 157:77–85.

Rich, P. M., D. D. Breshears, and A. B. White. 2008. Phenology of mixed woody-herbaceous ecosystems following extreme events: net and differential responses. Ecology 89:342–352.

Ripley, B. D. 1977. Modelling spatial patterns. Journal of the Royal Statistical Society Series B-Methodological 39:172–212.

Royer, P. D., N. S. Cobb, M. J. Clifford, C.-Y. Huang, D. D. Breshears, H. D. Adams, and J. Camilo Villegas. 2011. Extreme climatic event-triggered overstorey vegetation loss increases understorey solar input regionally: primary and secondary ecological implications. Journal of Ecology 99:714–723.

Rozas, V., and J. M. Olano. 2013. Environmental heterogeneity and neighbourhood interference modulate the individual response of *Juniperus thurifera* tree-ring growth to climate. Dendrochronologia 31:105–113.

Sánchez-Salguero, R., J. J. Camarero, M. Dobbertin, Á. Fernández-Cancio, A. Vilà-Cabrera, R. D. Manzanedo, M. A. Zavala, and R. M. Navarro-Cerrillo. 2013. Contrasting vulnerability and resilience to drought-induced decline of densely planted vs. natural rear-edge *Pinus nigra* forests. Forest Ecology and Management 310:956–967.

Saquete Ferrandiz, A., M. J. Lledo Solbes, A. Escarre Esteve, M. A. Ripoll Morales, and E. De-Simon Navarrete. 2006. Effects of site preparation with micro-basins on *Pinus halepensis* Mill. afforestations in a semiarid ombroclimate. Annals of Forest Science 63:15–22.

Sarkar, D. 2008. Lattice: multivariate data visualization with R. Springer, New York, New York, USA.

Sarris, D., D. Christodoulakis, and C. Korner. 2007. Recent decline in precipitation and tree growth in the eastern Mediterranean. Global Change Biology 13:1187–1200.

Sarris, D., R. Siegwolf, and C. Koerner. 2013. Inter- and intra-annual stable carbon and oxygen isotope signals in response to drought in Mediterranean pines. Agricultural and Forest Meteorology 168:59–68.

Schiller, G. 1972. Ecological factors affecting the growth of Aleppo pine in the southern Judean hills. Leaflet No. 44. [In Hebrew.] Agricultural Research Organization, Forest Division, Ilanot, Israel.

Schiller, G. 1977. Interrelations between site factors and performance of Aleppo pine in the Sha'ar ha'Gay forest. [Hebrew with English summary.] La-Yaaran 27:13–23.

Schiller, G. 1982. Significance of bedrock as a site factor for Aleppo pine. Forest Ecology and Management 4:213–223.

Schiller, G. 2000. Ecophysiology of *Pinus halepensis* Mill. and *P. brutia* Ten. Pages 51–65 *in* G. Ne'eman and L. Traubaud, editors. Ecology, biogeography and management of *Pinus halepensis* and *P. brutia* forest ecosystems in the Mediterranean Basin. Backhuys, Leiden, The Netherlands.

Schiller, G. 2013. Degeneration and premature mortality of *Pinus halepensis* in Israel following seeds importation from foreign ecosystems. [In Hebrew.] Ecology and Environment 4:167–175.

Schiller, G., and N. Atzmon. 2009. Performance of Aleppo pine (*Pinus halepensis*) provenances grown at the edge of the Negev desert: a review. Journal of Arid Environments 73:1051–1057.

Schiller, G., E. D. Ungar, S. Cohen, and N. Herr. 2010. Water use by Tabor and Kermes oaks growing in their respective habitats in the Lower Galilee region of Israel. Forest Ecology and Management 259:1018–1024.

Schiller, G., E. D. Ungar, S. Cohen, Y. Moshe, and N. Atzmon. 2009. Aspect effect on transpiration of *Pinus halepensis* in Yatir forest. [In Hebrew.] Yaar 11:14–19.

Schiller, G., E. D. Ungar, and Y. Cohen. 2002. Estimating the water use of a sclerophyllous species under an East-Mediterranean climate: I. Response of transpiration of *Phillyrea latifolia* L. to site factors. Forest Ecology and Management 170:117–126.

Schiller, G., E. D. Ungar, and A. Genizi. 2005. Is tree fate written in its tree rings? Characterization of trees in Kramim forest following the 1998/99 dry winter. [In Hebrew.] Yaar 7:18–25.

Schwinning, S. 2010. The ecohydrology of roots in rocks. Ecohydrology 3:238–245.

Shafran-Nathan, R., T. Svoray, and A. Perevolotsky. 2013. Continuous droughts' effect on herbaceous vegetation cover and productivity in rangelands: results from close-range photography and spatial analysis. International Journal of Remote Sensing 34:6263–6281.

Shimazaki, M., T. Sasaki, K. Hikosaka, and T. Nakashizuka. 2011. Environmental dependence of population dynamics and height growth of a subalpine conifer across its vertical distribution: an approach using high-resolution aerial photographs. Global Change Biology 17:3431–3438.

Stimson, H. C., D. D. Breshears, S. L. Ustin, and S. C. Kefauver. 2005. Spectral sensing of foliar water conditions in two co-occurring conifer species: *Pinus edulis* and *Juniperus monosperma*. Remote Sensing of Environment 96:108–118.

Suarez, M. L., L. Ghermandi, and T. Kitzberger. 2004. Factors predisposing episodic drought-induced tree mortality in *Nothofagus*–site, climatic sensitivity and growth trends. Journal of Ecology 92:954–966.

Svoray, T., and A. Karnieli. 2011. Rainfall, topography and primary production relationships in a semiarid ecosystem. Ecohydrology 4:56–66.

Syed, K. H., D. C. Goodrich, D. E. Myers, and S. Sorooshian. 2003. Spatial characteristics of thunderstorm rainfall fields and their relation to runoff. Journal of Hydrology 271:1–21.

Tucker, C. J. 1979. Red and photographic infrared linear combinations for monitoring vegetation. Remote Sensing of Environment 8:127–150.

Ungar, E. D., E. Rotenberg, N. Raz-Yaseef, S. Cohen, D. Yakir, and G. Schiller. 2013. Transpiration and annual water balance of Aleppo pine in a semiarid region: implications for forest management. Forest Ecology and Management 298:39–51.

Vacchiano, G., M. Garbarino, E. Borgogno Mondino, and R. Motta. 2012. Evidences of drought stress as a predisposing factor to Scots pine decline in Valle d'Aosta (Italy). European Journal of Forest Research 131:989–1000.

Venables, W. N., and B. D. Ripley. 2002. Modern applied statistics with S. Springer, New York, New York, USA.

Vicente-Serrano, S. M., T. Lasanta, and C. Gracia. 2010. Aridification determines changes in forest growth in *Pinus halepensis* forests under semiarid Mediterranean climate conditions. Agricultural and Forest Meteorology 150:614–628.

Vila-Cabrera, A., J. Martinez-Vilalta, L. Galiano, and J. Retana. 2013. Patterns of forest decline and regeneration across Scots pine populations. Ecosystems 16:323–335.

Vila-Cabrera, A., J. Martinez-Vilalta, J. Vayreda, and J. Retana. 2011. Structural and climatic determinants of demographic rates of Scots pine forests across the Iberian Peninsula. Ecological Applications 21:1162–1172.

Volcani, A., A. Karnieli, and T. Svoray. 2005. The use of remote sensing and GIS for spatio-temporal analysis of the physiological state of a semi-arid forest with respect to drought years. Forest Ecology and Management 215:239–250.

Weinstein-Evron, M., and S. Lev-Yadun. 2000. Palaeoecology of *Pinus halepensis* in Israel in the light of palynological and archaeobotanical data. Pages 119–130 *in* G. Ne'eman and L. Traubaud, editors. Ecology, biogeography and management of *Pinus halepensis* and *P. brutia* forest ecosystems in the Mediterranean Basin. Backhuys, Leiden, The Netherlands.

Weiss, J. L., C. L. Castro, and J. T. Overpeck. 2009. Distinguishing pronounced droughts in the southwestern United States: seasonality and effects of warmer temperatures. Journal of Climate 22:5918–5932.

Wickham, H. 2009. ggplot2: elegant graphics for data analysis. Springer, New York, New York, USA.

Worrall, J. J., L. Egeland, T. Eager, R. A. Mask, E. W. Johnson, P. A. Kemp, and W. D. Shepperd. 2008. Rapid mortality of *Populus tremuloides* in southwestern Colorado, USA. Forest Ecology and Management 255:686–696.

Wulder, M. A., S. M. Ortlepp, J. C. White, and S. Maxwell. 2008. Evaluation of Landsat-7 SLC-off image products for forest change detection. Canadian Journal of Remote Sensing 34:93–99.

Yakir, H., and E. Morin. 2011. Hydrologic response of a semi-arid watershed to spatial and temporal characteristics of convective rain cells. Hydrology and Earth System Sciences 15:393–404.

Yuhas, A. N., and L. A. Scuderi. 2009. MODIS-derived NDVI characterisation of drought-induced evergreen dieoff in western North America. Geographical Research 47:34–45.

Zaady, E., M. Shachak, and Y. Moshe. 2001. Ecological approach for afforestation in arid regions of the northern Negev Desert, Israel. Pages 219–238 *in* D. K. Vajpeyi, editor. Deforestation, environment, and sustainable development: a comparative analysis. Praeger, Westport, Connecticut, USA.

Zuur, A. F., E. N. Ieno, N. J. Walker, A. A. Saveliev, and G. M. Smith. 2009. Mixed effects models and extensions in ecology with R. Springer-Verlag, New York, New York, USA.